# From Silicene to Half-Silicane by Hydrogenation

Jinglan Qiu,[†] Huixia Fu,[†] Yang Xu,[†,‡] Qing Zhou,[‡] Sheng Meng,[†] Hui Li,[†] Lan Chen,[*,†] and Kehui Wu[*,†,§]

[†]Institute of Physics, Chinese Academy of Sciences, Beijing 100190, China, [‡]Department of Physics, Yunnan University, Kunming 650091, China, and [§]Collaborative Innovation Center of Quantum Matter, Beijing 100871, China

ABSTRACT Graphane is graphene fully hydrogenated from both sides, forming a 1×1 structure, where all C atoms are in sp³ configuration. In silicene, the Si atoms are in a mixed sp²/sp³ configuration; it is therefore natural to imagine a silicane structure analogous to graphane. However, a monatomic silicene sheet grown on substrates generally reconstructs into different phases, and only partially hydrogenated silicene with reconstructions had been reported before. In this work, we produce half-silicane, where one Si sublattice is fully H-saturated and the other sublattice is intact, forming a perfect 1×1 structure. By hydrogenating various silicene phases on a Ag(111) substrate, we found that only the $(2\sqrt{3}\times2\sqrt{3})R30°$ phase can produce half-silicane. Interestingly, this phase was previously considered to be a highly defective or incomplete silicene structure. Our results indicate that the structure of the $(2\sqrt{3}\times2\sqrt{3})R30°$ phase involves a complete silicene-1×1 lattice instead of defective fragments, and the formation mechanism of half-silicane was discussed with the help of first-principles calculations.
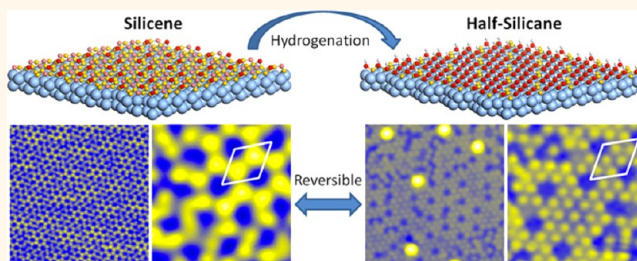
KEYWORDS: silicene · silicane · hydrogenation · scanning tunneling microscopy

Silicene, a monatomic layer of silicon atoms tightly packed into a low-buckled honeycomb lattice, is attracting increasing scientific interest due to its fascinating electronic properties and potential applications.[1−6] It is expected to be a new massless Dirac Fermion system like graphene,[7,8] but with additional benefits such as a large spin−orbit coupling gap[1] and a strong response to an external electric field.[3] In the past few years, epitaxial synthesis of silicene has been demonstrated on various supporting substrates, like Ag(111),[7−18] ZrB₂(0001)/Si(111),[19,20] Ir(111),[21] and MoS₂,[22] predominantly on Ag(111). The monolayer silicene on the Ag(111) substrate exhibits a variety of superstructures, such as 4×4, $(\sqrt{13}\times\sqrt{13})$-R13.9°, and $(2\sqrt{3}\times2\sqrt{3})R30°$ with respect to the Ag(111)-1×1 lattice[7,9−17] and $(\sqrt{3}\times\sqrt{3})R30°$ with respect to the Si(111)-1×1 lattice.[10,15−17] Among these phases, only the $(2\sqrt{3}\times2\sqrt{3})R30°$ phase can exist in a single phase and cover the entire Ag(111) surface uniformly (the 4×4 phase usually coexists with the $(\sqrt{13}\times\sqrt{13})R13.9°$ phase). However, compared with the ordered 4×4 phase, the $(2\sqrt{3}\times2\sqrt{3})R30°$ phase appears very disordered and defective in the scanning tunneling microscope (STM) image.[10] It has an arrangement of ordered areas with $(2\sqrt{3}\times2\sqrt{3})R30°$ structure surrounded by apparently defective areas. Therefore, there is a strong debate about whether it should be regarded as a well-defined phase of silicene.[23] There are also increasing debates on whether the $(2\sqrt{3}\times2\sqrt{3})R30°$ is a pure silicon phase or if it should include a Si−Ag alloy.[24,25] Meanwhile, recently Tao et al. reported the first field-effect transistor devices based on monolayer silicene prepared on and then peeled off from a Ag(111) substrate.[26] They selected 4×4 and $(2\sqrt{3}\times2\sqrt{3})R30°$ phases as the starting materials. As a result, both devices have basically the same properties. It is intriguing because if the 4×4 is an ordered phase while $(2\sqrt{3}\times2\sqrt{3})R30°$ is severely defective, then their transport behaviors, including carrier density and mobility, should be very different.
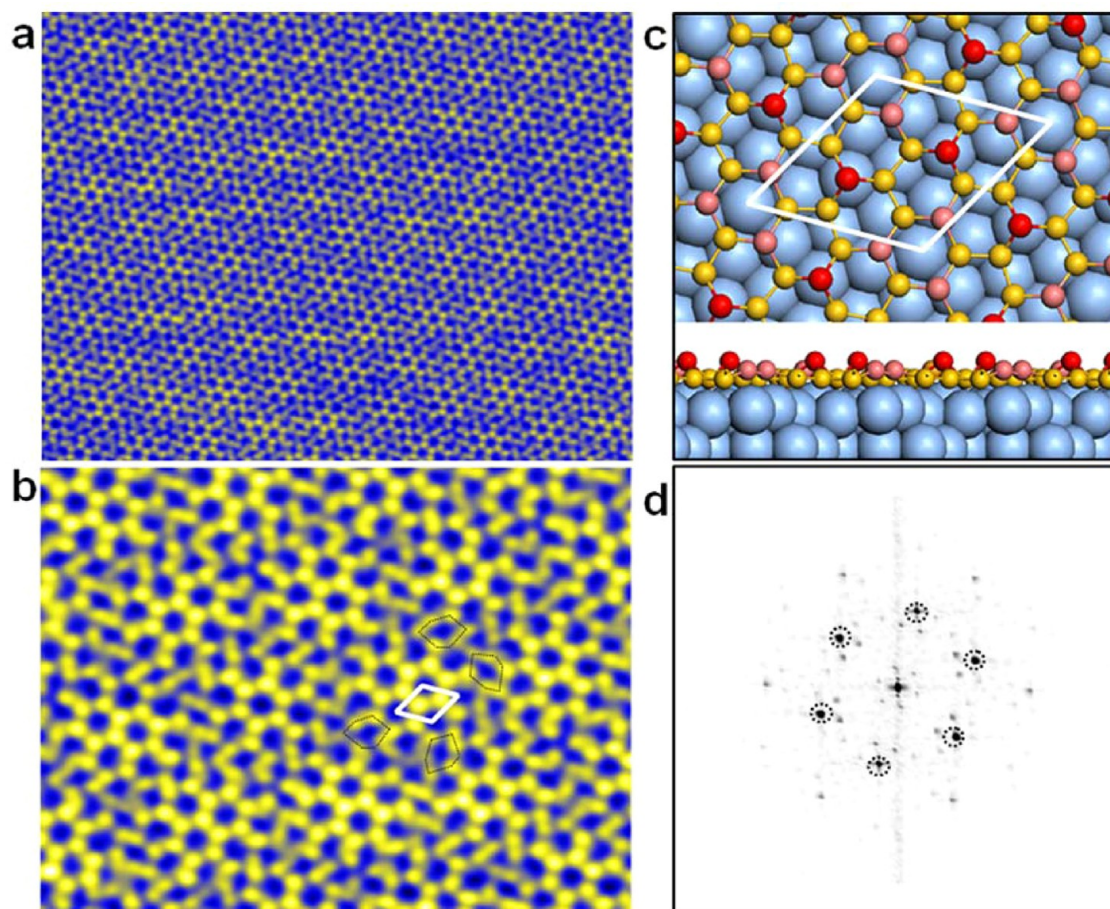
To understand these issues, it is of key importance to understand the atomic structure of the $(2\sqrt{3}\times2\sqrt{3})R30°$ silicene phase. In this paper, we report that, by hydrogenation, the hidden silicon lattice of $(2\sqrt{3}\times2\sqrt{3})R30°$ silicene can be disclosed. The STM images show a well-ordered,

Figure 1. Structures of the silicene $(2\sqrt{3}\times2\sqrt{3})R30°$ phase on the Ag(111) surface. **(a)** Large-area STM image (42×32 nm^2, $V_{tip} = 1.50$ V, $I_{set-point} = 40.0$ pA) of the monolayer silicene $(2\sqrt{3}\times2\sqrt{3})R30°$ phase. **(b)** High-resolution STM image (16×12 nm^2, $V_{tip} = 1.50$ V, $I_{set-point} = 40.0$ pA) shows a few complete honeycomb rings with $(2\sqrt{3}\times2\sqrt{3})R30°$ structure. The white rhombus represents the unit cell of the $(2\sqrt{3}\times2\sqrt{3})R30°$ phase. Four distorted hexagons around the complete honeycomb rings are marked by black dotted lines. **(c)** Top and side views of the structural model of the silicene $(2\sqrt{3}\times2\sqrt{3})R30°$ phase. The large and small balls represent the Ag and Si atoms, respectively. The different colors of small balls indicate the different buckling degrees of Si atoms. The white rhombus represents the unit cell of the $(2\sqrt{3}\times2\sqrt{3})R30°$ phase. **(d)** Result of fast FFT of (a). The $(2\sqrt{3}\times2\sqrt{3})R30°$ spots are marked by black dotted circles.

pristine silicene-1×1 lattice after hydrogenation at room temperature, indicating that the original silicene $(2\sqrt{3}\times2\sqrt{3})R30°$ superstructure consists of a complete monolayer silicene lattice. The observed hydrogenated structure corresponds to half-silane, where one Si sublattice is fully H-saturated and the other sublattice is intact, forming a perfect 1×1 structure. Our experiment also solves the debate on whether monolayer silicene on Ag is an alloy phase because the 1×1 structure is so simple that one can hardly construct an alloy model to involve Ag atoms. Moreover, it also answers the question of why the devices based on 4×4 and $(2\sqrt{3}\times2\sqrt{3})R30°$ are the same because, indeed, they are not different once the substrate is removed.

RESULTS AND DISCUSSION

Figure 1a shows a large-area STM topographic image of a monolayer $(2\sqrt{3}\times2\sqrt{3})$ silicene, which fully covers the whole Ag(111) substrate surface in a single phase. Two sets of periods can be found in the

image: the small one with $(2\sqrt{3}\times2\sqrt{3})$ periodicity and the large period of about 3.8 nm. The high-resolution STM image in Figure 1b shows locally a few complete honeycomb rings with a period of 1.0 nm in perfect area, indicating it is a $(2\sqrt{3}\times2\sqrt{3})R30°$ structure. The fast Fourier transformation (FFT) of the STM image (Figure 1d) shows the $(2\sqrt{3}\times2\sqrt{3})R30°$ spots marked by the black circles. We also observe six spots surrounding the $(0, 0)$ and each $(2\sqrt{3}, 2\sqrt{3})$ spot, which correspond to the large period in the STM image.

The perfect area with complete honeycomb rings can be understood by a model where a monolayer silicene lattice overlaps on Ag(111) with a 10.9° in-plane rotation with respect to the Ag[110] azimuth,[27] shown in Figure 1c. However, the areas surrounding the perfect area appear disordered. Our early work proposed that the origin of the disordered areas is due to mismatch between the silicene lattice and Ag(111), which results in fragments of monolayer silicene.[10] Liu *et al.* considered the $(2\sqrt{3}\times2\sqrt{3})R30°$ superstructure

as a patchwork of fragmented silicene pieces, which is inherently highly defective and inhomogeneous.[23] However, carefully inspecting the disordered area, one can find hidden order everywhere. Around a dark site, there are always six spots, not more and not less. Connecting these six spots will result in a hexagon (as shown in Figure 1b), albeit the hexagon is obviously distorted compared with the perfect ones in the ordered center. Some of these six spots appear darker, which is the reason why the defective area appears darker than the perfect area. Jamgotchian *et al.* suggested recently that the disordered areas are related to a local relaxation of epitaxial strain and appeared as shrunk hexagons in the STM image.[28] In other words, despite the apparent disorder given by the STM images, the silicene film retains a continuous honeycomb lattice with only local and periodic deformations. On the other hand, there are some researchers who regard this phase as the Si−Ag alloy.[24,25] So far, there is still no conclusion for these issues. The difficulty of explanation is that the buckling degree of Si atoms in silicene grown on Ag(111) is largely rearranged due to the strong Si−Ag interactions, so only a small number of the upper buckled Si atoms can be resolved in the STM image, while the others are hidden. In our recent work, we have shown that adsorption of hydrogen atoms on silicene can change the buckling arrangement of Si atoms.[29] In this study, we explore hydrogenation of the $(2\sqrt{3}\times2\sqrt{3})R30°$ phase to give more information about the atomic structure.

Similar to the hydrogenated silicene 4×4 phase,[29] the fully hydrogenated $(2\sqrt{3}\times2\sqrt{3})R30°$ phase also exhibits an ordered structure. From the STM image of Figure 2a, we find that the ordered structure consists of hexagonal close-packed (hcp) spots (some big bright protrusions in the image are due to contaminations during H adsorption). The hcp spots have a lattice period of about 3.8 Å, identical to the lattice constant of silicene-1×1. The FFT on the STM image of the hydrogenated $(2\sqrt{3}\times2\sqrt{3})R30°$ phase results in six spots corresponding to silicene-1×1, as shown in the inset of Figure 2a. Another obvious feature of the film is the black holes corresponding to missing single atom sites. Detailed analysis of the hole sites gives us rich structural information. First, most of the hole sites are arranged in a periodically ordered $\sqrt{7}\times\sqrt{7}$ pattern with respect to silicene-1×1, as shown by the white rhombus in Figure 2a,b. The FFT image also shows the six spots corresponding to a $\sqrt{7}\times\sqrt{7}$ superstructure (inset of Figure 2a). Notably, the $\sqrt{7}\times\sqrt{7}$ periodicity with respect to silicene-1×1 is identical to a $(2\sqrt{3}\times2\sqrt{3})R30°$ periodicity with respect to Ag(111)-1×1. Besides the ordered holes, there are another two types of holes shown in Figure 2a,b. The second type is formed by two holes sitting side by side, and the third type consists of a bright spot at the center surrounded by three holes.
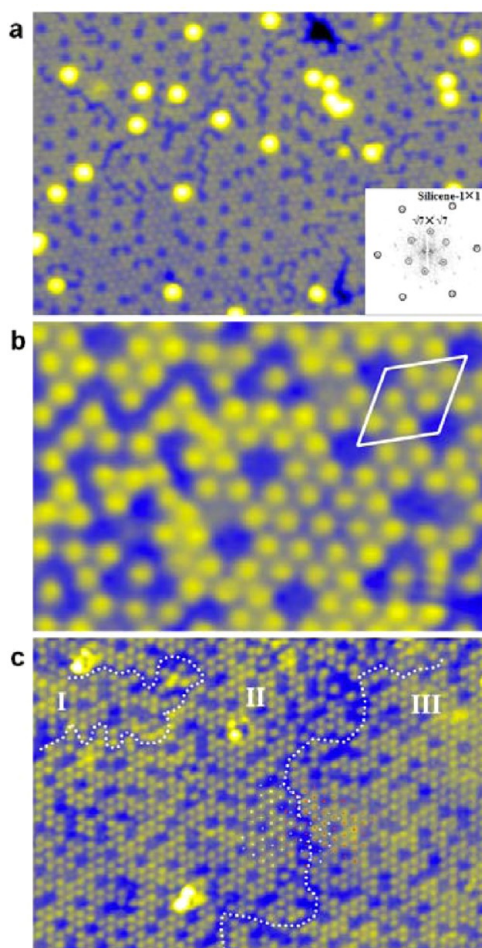
Figure 2. Full hydrogenation of the silicene $(2\sqrt{3}\times2\sqrt{3})R30°$ phase on Ag(111). (a) STM image (17×12 nm^2, V_{tip} = 0.50 V, $I_{set\text{-}point}$ = 430.0 pA) of the fully hydrogenated silicene $(2\sqrt{3}\times2\sqrt{3})R30°$ phase. The inset is the result of FFT of (a), showing six spots corresponding to silicene-1×1 lattice. **(b)** High-resolution STM image (5×4 nm^2, V_{tip} = 0.20 V, $I_{set\text{-}point}$ = 281.0 pA) of the hydrogenated $(2\sqrt{3}\times2\sqrt{3})R30°$ phase. The white rhombus marks the periodically ordered hole sites with $\sqrt{7}\times\sqrt{7}$ structure with respect to the silicene 1×1 lattice, which agrees well with the $\sqrt{7}\times\sqrt{7}$ spots observed in the inset of (a). **(c)** STM image (15×10 nm^2, V_{tip} = 0.43 V, $I_{set\text{-}point}$ = 80.0 pA) of the hydrogenated silicene $(2\sqrt{3}\times2\sqrt{3})R30°$ phase shows three domains (marked by I, II, and III). The domain boundaries are labeled by white dotted lines. The small white and red dots correspond to the lattice of the bright spots in II and III domains, respectively. One lattice is exactly located in the hollow site of the other lattice.

We name the above three types of holes mono, double, and triple holes, respectively.

Free-standing silicene is known to be a low-buckled structure with hybridization between sp^2 and sp^3 due to the large Si−Si interatomic distance that weakens the $\pi-\pi$ overlap.[1] The bonding of H on Si is expected to favor sp^3 hybridization, which will increase the out-of-plane buckling of Si in the direction of the bonded hydrogen.[30] Previous theoretical works proposed that chairlike configuration with hydrogen atoms attached to two sublattices from the two opposite sides of the silicene sheet is the most stable for free-standing
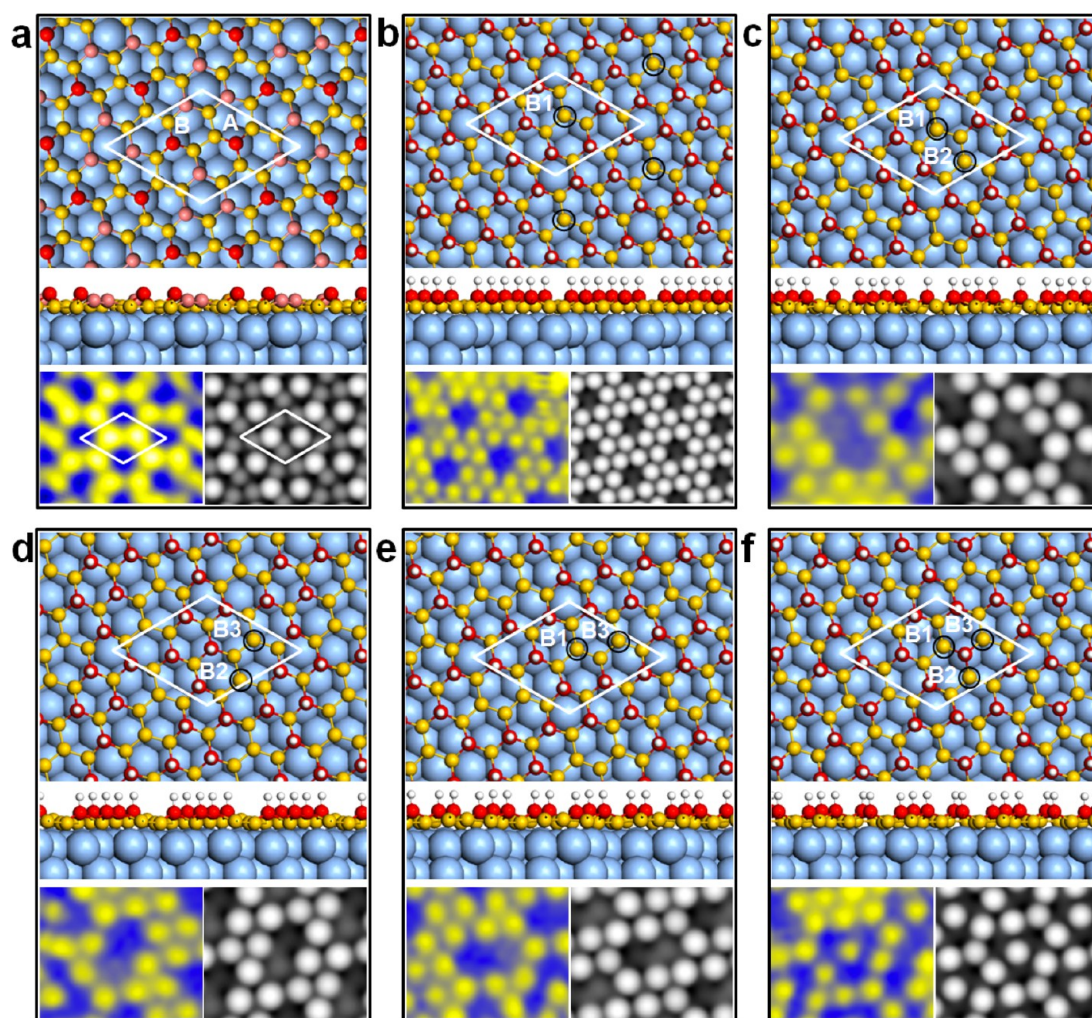
Figure 3. Calculated structures of hydrogenated silicene-($2\sqrt{3}\times2\sqrt{3}$) with different holes. (a−f) Top panel: Top and side views of DFT-calculated structure model. Bottom panel: experimental (left) and simulated (right) STM images. The white rhombus represents the unit cell of the ($2\sqrt{3}\times2\sqrt{3}$)$R30°$ phase. (a) Silicene ($2\sqrt{3}\times2\sqrt{3}$)$R30°$ phase before hydrogenation. The two upper-buckled Si atoms (named A and B) in the unit cell correspond to the bright spots in the STM image and belong to two different sublattices. (b) Hydrogenated silicene ($2\sqrt{3}\times2\sqrt{3}$)$R30°$ phase with a mono hole in one unit cell. The Si atom without hydrogenation is marked by the black circle and is named B1. (c−e) Three identical conformations of hydrogenated silicene with double holes in one unit cell. The Si atoms without hydrogenation are marked by black circles and named B1, B2, and B3. (f) Hydrogenated silicene with triple holes in one unit cell. In this structure, all of the B1, B2, and B3 atoms are not hydrogenated while the A atom bonds a H atom.

silicene.[31] However, when the Ag(111) substrate is taken into account, only one side of silicene is accessible to hydrogenation. Recently, we have studied the hydrogenation of silicene-4×4 by STM and density functional theory (DFT) calculations.[29] Our results showed a perfectly ordered γ-4×4 superstructure after hydrogenation of silicene-4×4. Combined with the STM images and DFT calculations, we also found that H atoms basically react with the upper-buckled Si atoms.

In the following discussions, we will show how the original ($2\sqrt{3}\times2\sqrt{3}$)$R30°$ superstructure of silicene on Ag(111) can result in a hydrogenated hcp structure as well as the characteristic holes. If it is assumed that the ($2\sqrt{3}\times2\sqrt{3}$)$R30°$ phase is the single sheet of silicene on Ag(111) (the model is shown in Figures 1c and 3a), then the bright protrusions observed in the STM images are the most upper-buckled Si atoms directly

on top of Ag atoms. It is quite interesting that there are two most upper-buckled Si atoms (we named A and B) in each ($2\sqrt{3}\times2\sqrt{3}$)$R30°$ unit cell, which belong to two different sublattices, respectively. Experimentally, when enough H atoms are adsorbed on the surface, we obtain a 1×1 hcp lattice, which should correspond to a complete sublattice, either A or B sublattice that reacts with H atoms. We suppose that the B sublattice is terminated by H atoms, as shown in Figure 3b. During this process, the Si atom in the A site, which is one of the two most upper-buckled Si atoms in each ($2\sqrt{3}\times2\sqrt{3}$)$R30°$ unit cell, is pushed downward, and the three surrounding Si atoms are shifted upward and terminated by H atoms. For the convenience of discussion, we named these three Si atoms as B1, B2, and B3. To explain our observation of mono, double, and triple holes, we propose that they correspond to one,

TABLE 1. Total Energy, E_{tot} (eV), and Binding Energy, E_b (eV/H), of Hydrogen Atom Calculated by DFT Calculations[a]

structure	E_{tot} (eV)	E_b (eV/H)
Si($\sqrt{7}\times\sqrt{7}$)/Ag($2\sqrt{3}\times2\sqrt{3}$)	−233.877	
Si($\sqrt{7}\times\sqrt{7}$)/Ag($2\sqrt{3}\times2\sqrt{3}$)-7H	−259.808	−2.596
Si($\sqrt{7}\times\sqrt{7}$)/Ag($2\sqrt{3}\times2\sqrt{3}$)-6H	−256.323	−2.633
Si($\sqrt{7}\times\sqrt{7}$)/Ag($2\sqrt{3}\times2\sqrt{3}$)-5H$_{a1}$	−252.726	−2.661
Si($\sqrt{7}\times\sqrt{7}$)/Ag($2\sqrt{3}\times2\sqrt{3}$)-5H$_{a2}$	−252.728	−2.662
Si($\sqrt{7}\times\sqrt{7}$)/Ag($2\sqrt{3}\times2\sqrt{3}$)-5H$_{a3}$	−252.723	−2.661
Si($\sqrt{7}\times\sqrt{7}$)/Ag($2\sqrt{3}\times2\sqrt{3}$)-5H$_b$	−252.719	−2.660

[a] For (1) clean silicene ($2\sqrt{3}\times2\sqrt{3}$)R30° structure; (2) fully hydrogenated silicene without defects named Si($\sqrt{7}\times\sqrt{7}$)/Ag($2\sqrt{3}\times2\sqrt{3}$)-7H; (3) hydrogenated silicene with mono hole structure, which is shown in Figure 3b, and named Si($\sqrt{7}\times\sqrt{7}$)/Ag($2\sqrt{3}\times2\sqrt{3}$)-6H; (4) hydrogenated silicene with double hole structures, which are shown in Figure 3c−e, and named Si($\sqrt{7}\times\sqrt{7}$)/Ag($2\sqrt{3}\times2\sqrt{3}$)-5H$_{a1}$, Si($\sqrt{7}\times\sqrt{7}$)/Ag($2\sqrt{3}\times2\sqrt{3}$)-5H$_{a2}$, Si($\sqrt{7}\times\sqrt{7}$)/Ag($2\sqrt{3}\times2\sqrt{3}$)-5H$_{a3}$; (5) hydrogenated silicene with triple hole structure, which is shown in Figure 3f, and named Si($\sqrt{7}\times\sqrt{7}$)/Ag($2\sqrt{3}\times2\sqrt{3}$)-5H$_b$.

two, or three (B1, B2, B3) Si atoms without hydrogenation, respectively (for triple holes, the bright spot at the center should be the A atom terminated by a hydrogen atom). This occurs because they are the nearest neighbor of the originally most upper-buckled Si atom in the A site, and thus it is difficult for them to buckle up. To confirm this picture, we performed DFT calculations on the structures of fully hydrogenated silicene (Si($\sqrt{7}\times\sqrt{7}$)/Ag($2\sqrt{3}\times2\sqrt{3}$)-7H), hydrogenated silicene with a mono hole (Si($\sqrt{7}\times\sqrt{7}$)/Ag($2\sqrt{3}\times2\sqrt{3}$)-6H), double holes (Si($\sqrt{7}\times\sqrt{7}$)/Ag($2\sqrt{3}\times2\sqrt{3}$)-5H$_a$), and triple holes (Si($\sqrt{7}\times\sqrt{7}$)/Ag($2\sqrt{3}\times2\sqrt{3}$)-5H$_b$). The relaxed structures are shown in Figure 3b−f, while the total energy and binding energy of H are shown in Table 1. From the calculated results, we find that the binding energy of the hydrogen atom of Si($\sqrt{7}\times\sqrt{7}$)/Ag($2\sqrt{3}\times2\sqrt{3}$)-7H (E_b = −2.596 eV) is the lowest among all the structures. It means that fully hydrogenated silicene with a 1×1 lattice is not the most stable structure; instead, one or two Si atoms without hydrogenation in one $\sqrt{7}\times\sqrt{7}$ unit cell will happen spontaneously to preserve a stable hydrogenated silicene structure. This is in accord with the observation of holes in STM images very well. The slight probability that the (B1, B2, B3) atoms react with H atoms may result from the influence of the originally most upper-buckled atom A.

For hydrogenated silicene with a mono hole in one unit cell, each one of the three Si atoms (B1, B2, and B3) has the same probability to not react with a H atom, so the exact positions of the holes in the unit cell of a $\sqrt{7}\times\sqrt{7}$ superstructure have a random shift in three directions with a distance of a, where a is the lattice constant of silicene-1×1. From this point of view, we can now explain why the $\sqrt{7}\times\sqrt{7}$ superstructure of mono holes in the STM image is imperfect. The hydrogenated silicene with double holes in one unit cell correspond to two of the three Si atoms (B1, B2, and B3) without

hydrogenation. There should be three identical conformations with orientations separated by 120° with respect to each other (shown in Figure 3c−e), and the binding energy of the H atoms for the three structures are almost the same as that in our calculations (Table 1). This feature also can be observed in STM images (Figure 2a and Figure 3c−e). The hydrogenated silicene with triple holes corresponds to all of the B1, B2, and B3 atoms being nonhydrogenated, but the A atom bonds a H atom (Figure 3f). In our calculations, the total energy and the binding energy of H atoms for this structure are almost the same as that of the hydrogenated silicene with double holes (Table 1), indicating the similar stability. Moreover, the simulated STM images of the hydrogenated silicene with different holes coincide with the STM images very well (shown in Figure 3a−f), which proves the correctness of our model.

With the hydrogenation mechanism and structural model discussed above, there should be a same possibility for the two different sublattices of silicene to be hydrogenated.[29] As a result, the hydrogenated silicene-($2\sqrt{3}\times2\sqrt{3}$)R30° will separate into different domains, where either the A sublattice or B sublattice is hydrogenated. In our experiment, we observed such features. The STM image of Figure 2c shows a hydrogenated silicene surface which appears at first sight to have a well-ordered single domain. However, by careful inspection, one notices that there are three domains, separated by two domain boundaries that are labeled by white dotted lines. We marked the positions of bright spots in neighboring domains (both hcp lattices), and one can note that one hcp lattice is exactly located in the hollow site of the other hcp lattice, which is exactly what we expect from the above sublattice hydrogenation picture: A and B sublattices are located in the hollow sites of each other.

The observation of a continuous, pristine 1×1 lattice of silicene after hydrogenation strongly suggests that the ($2\sqrt{3}\times2\sqrt{3}$)R30° phase is a continuous silicene film on Ag(111). The apparently defective area observed in the STM images of a clean ($2\sqrt{3}\times2\sqrt{3}$)R30° phase does not consist of fragments of silicene[10,23] but simply results from the lower-buckled Si atoms that are not resolved by STM. The possibility that the ($2\sqrt{3}\times2\sqrt{3}$)R30° phase is the Si−Ag alloy[24,25] is also ruled out because the simple 1×1 lattice after hydrogenation is unlikely to be explained by any complicated alloy model, and our pure silicene model can perfectly explain the observed 1×1 structure as well as the mono, double, and triple hole defects after hydrogenation.

Previous theoretical calculations suggested intriguing properties in hydrogenated silicene, for example, a large gap (∼3 eV) opening[31,32] and interesting ferromagnetic[33] and optoelectronic properties.[34] The local interaction between Si and Ag atoms causes the rearrangements of buckling of Si atoms and also influences the results of hydrogenation. For silicene-4×4, the full hydrogenation
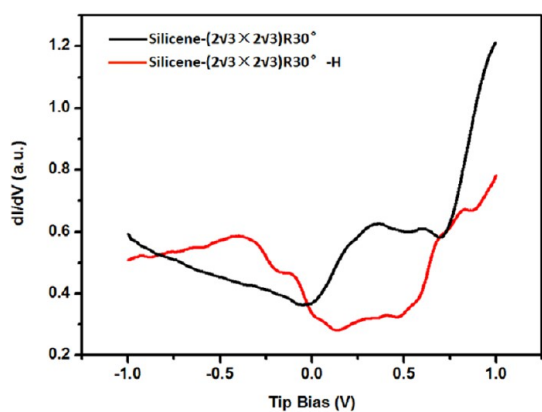
Figure 4. STS results of silicene-$(2\sqrt{3}\times2\sqrt{3})R30°$ before (black curve) and after (red curve) hydrogenation.

results in only 7 H atoms in one unit cell (7/9 monolayer) but no change of the structural periodicity.[29] For the $(2\sqrt{3}\times2\sqrt{3})R30°$ phase, the whole structure changes to a 1×1 periodicity, and the density of H atoms bonded to Si (about 6/7 monolayer) is much higher than 4×4 while still less than the ideal free-standing 1×1 due to the existence of periodic defects. To get perfect fully hydrogenated silicene-1×1 lattice, the interaction between Si and the substrate should be modified, which is also a next stage of the investigation on silicene.

The hydrogenation on silicene should largely influence the electronic properties of silicene, which is similar to those of the carbon analogue.[35] We performed scanning tunneling spectroscopy (STS) measurements on hydrogenated silicene. The STS results of silicene-$(2\sqrt{3}\times2\sqrt{3})R30°$ before and after hydrogenation are shown in Figure 4. We find that the density of states of hydrogenated silicene at the energy range from the Fermi level to 0.6 eV is largely decreased compared with that of silicene, which may stem from the gap opening of silicene after hydrogenation. The shoulders at −0.1 and +0.7 eV may correspond to the conductance band and valence band of hydrogenated silicene, respectively. (It is noteworthy that the bias was applied on the tip.) We must point out that there are strong interactions between silicene and the Ag(111) surface, which may disturb the original electronic properties of silicene. That is why the differential conductance of hydrogenated silicene that we observed from the Fermi level to 0.6 eV in STS is not zero.

Finally, we exploited the dehydrogenation process. It is remarkable that the fully hydrogenated silicene sheet can be completely restored to its original state by annealing the sample to a moderate temperature of about 450 K. As is shown in Figure 5, the complete honeycomb rings and defective areas with twisted
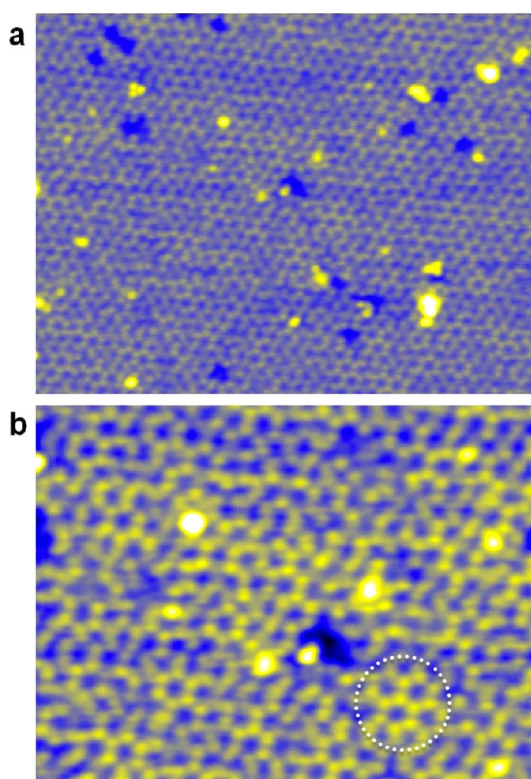
Figure 5. Dehydrogenation of silicene $(2\sqrt{3}\times2\sqrt{3})R30°$ phase on Ag(111). (a) STM image (38×27 nm^2, V_{tip} = 1.60 V, $I_{set\text{-}point}$ = 40.0 pA) of the hydrogenated silicene $(2\sqrt{3}\times2\sqrt{3})R30°$ phase after dehydrogenation. (b) High-resolution STM image (20×15 nm^2, V_{tip} = 1.60 V, $I_{set\text{-}point}$ = 40.0 pA) shows complete honeycomb rings marked by a white dotted circle.

honeycombs in the silicene $(2\sqrt{3}\times2\sqrt{3})R30°$ phase are completely restored after hydrogen desorption. The easily reversible hydrogenation of monolayer silicene suggests that silicene may be useful for controllable hydrogen storage.

CONCLUSIONS

In summary, we studied hydrogenation of silicene-$(2\sqrt{3}\times2\sqrt{3})R30°$ by STM and DFT calculations. The fully hydrogenated silicene-$(2\sqrt{3}\times2\sqrt{3})R30°$ produces a half-silicane. Compared with silicane or graphane, half-silicane may possess unique electronic properties that remain to be explored. Our results also suggest that silicene with a $(2\sqrt{3}\times2\sqrt{3})R30°$ superstructure is a complete monolayer silicene film, which does not involve lattice defects or alloy with Ag, and thus clarifies these debated issues. Our finding also suggests that the $(2\sqrt{3}\times2\sqrt{3})R30°$ phase may be a promising silicene phase for device applications, as this phase is easy to prepare, with high quality, and can cover the entire substrate surface uniformly.

METHODS

Experiments were carried out in a home-built low-temperature STM with a base pressure of 1×10^{-10} mbar. The single-crystal

Ag(111) surface was cleaned *in situ* by repeated cycles of Ar$^+$ ion sputtering followed by annealing to about 900 K. Silicon was evaporated from a heated wafer ($T \approx 1300$ K) onto the Ag(111)

substrate held at 500 K. Hydrogen adsorption was performed by exposing the sample at room temperature to a high-purity H_2 gas (pressures ranging from 1×10^{-5} to 1×10^{-4} Pa) cracked by a hot tungsten filament which was heated to about 2000 K. Then the sample was *in situ* transferred to the STM chamber for scanning without breaking the vacuum. All STM experiments were carried out at 77 K, and the bias voltage is defined as the tip bias with respect to the sample. Processing of the STM images was carried out with the WSxM software. The STS data were acquired using a lock-in amplifier by applying a small sinusoidal modulation to the tip bias voltage (typically 10 mV at 676 Hz). Calibration of the STS spectra was achieved by scanning a clean Ag(111) surface before and after scanning silicene and hydrogenated silicene.

Density functional theory calculations were performed using projector-augmented wave pseudopotentials in conjunction with the Perdew−Burke−Ernzerhof[36] function and plane-wave basis set with an energy cutoff at 250 eV. In the calculation, the $(\sqrt{7} \times \sqrt{7})$ supercells of silicon film on the five-layer $(2\sqrt{3} \times 2\sqrt{3})$ Ag(111) surface with the lattice constant of 10.01 Å were chosen. All the structures were fully relaxed with the bottom two layers of Ag atoms fixed. The vacuum region of more than 15 Å in the Z direction was applied, which is sufficiently large to eliminate the artificial periodic interaction, and the Brillouin zone is sampled by $5 \times 5 \times 1$ Monkhorst−Pack k-mesh. The geometries of multilayer silicene/Ag(111) systems were optimized until the force on each atom is less than 0.04 eV/Å. All the calculations are performed with Vienna ab initio simulation package.[37]

Conflict of Interest: The authors declare no competing financial interest.

REFERENCES AND NOTES

1. Liu, C. C.; Feng, W.; Yao, Y. G. Quantum Spin Hall Effect in Silicene and Two-Dimensional Germanium. *Phys. Rev. Lett.* **2011**, *107*, 076802.
2. Drummond, N. D.; Zolyomi, V.; Falko, V. I. Electrically Tunable Band Gap in Silicene. *Phys. Rev. B: Condens. Matter Mater. Phys.* **2012**, *85*, 075423.
3. Ezawa, M. Valley-Polarized Metals and Quantum Anomalous Hall Effect in Silicene. *Phys. Rev. Lett.* **2012**, *109*, 055502.
4. Ni, Z.; Liu, Q.; Tang, K.; Zheng, J.; Zhou, J.; Qin, R.; Gao, Z.; Yu, D.; Lu, J. Tunable Bandgap in Silicene and Germanene. *Nano Lett.* **2012**, *12*, 113–118.
5. Takagi, N.; Lin, C. L.; Kawahara, K.; Minamitani, E.; Tsukahara, N.; Kawai, M.; Arafune, R. Silicene on Ag(111): Geometric and Electronic Structures of a New Honeycomb Material of Si. *Prog. Surf. Sci.* **2015**, *90* (1), 1–20.
6. Oughaddou, H.; Enriquez, H.; Tchalala, M. R.; Yildirim, H.; Mayne, A. J.; Bendounan, A.; Dujardin, G.; Ali, M. A.; Kara, A. Silicene, a Promising New 2D Material. *Prog. Surf. Sci.* **2015**, *90* (1), 46–83.
7. Vogt, P.; De Padova, P.; Quaresima, C.; Avila, J.; Frantzeskakis, E.; Asensio, M. C.; Resta, A.; Ealet, B.; Le Lay, G. Silicene: Compelling Experimental Evidence for Graphenelike Two-Dimensional Silicon. *Phys. Rev. Lett.* **2012**, *108*, 155501.
8. Chen, L.; Liu, C. C.; Feng, B. J.; He, X. Y.; Cheng, P.; Ding, Z. J.; Meng, S.; Yao, Y. G.; Wu, K. H. Evidence for Dirac Fermions in a Honeycomb Lattice Based on Silicon. *Phys. Rev. Lett.* **2012**, *109*, 056804.
9. Jamgotchian, H.; Colignon, Y.; Hamzaoui, N.; Ealet, B.; Hoarau, J. Y.; Aufray, B.; Bibérian, J. P. Growth of Silicene Layers on Ag(111): Unexpected Effect of the Substrate Temperature. *J. Phys.: Condens. Matter* **2012**, *24*, 172001.
10. Feng, B. J.; Ding, Z. J.; Meng, S.; Yao, Y. G.; He, X. Y.; Cheng, P.; Chen, L.; Wu, K. H. Evidence of Silicene in Honeycomb Structures of Silicon on Ag(111). *Nano Lett.* **2012**, *12*, 3507–3511.
11. Chiappe, D.; Grazianetti, C.; Tallarida, G.; Fanciulli, M.; Molle, A. Local Electronic Properties of Corrugated Silicene Phases. *Adv. Mater.* **2012**, *24*, 5088–5093.
12. Lin, C. L.; Arafune, R.; Kawahara, K.; Tsukahara, N.; Minamitani, E.; Kim, Y.; Takagi, N.; Kawai, M. Structure of Silicene Grown on Ag(111). *Appl. Phys. Express* **2012**, *5*, 045802.
13. Enriquez, H.; Vizzini, S.; Kara, A.; Lalmi, B.; Oughaddou, H. Silicene Structures on Silver Surfaces. *J. Phys.: Condens. Matter* **2012**, *24*, 314211.
14. Liu, Z. L.; Wang, M. X.; Xu, J. P.; Ge, J. F.; Le Lay, G.; Vogt, P.; Qian, D.; Gao, C. L.; Liu, C.; Jia, J. F. Various Atomic Structures of Monolayer Silicene Fabricated on Ag(111). *New J. Phys.* **2014**, *16*, 075006.
15. Chen, L.; Li, H.; Feng, B. J.; Ding, Z. J.; Qiu, J. L.; Cheng, P.; Wu, K. H.; Meng, S. Spontaneous Symmetry Breaking and Dynamic Phase Transition in Monolayer Silicene. *Phys. Rev. Lett.* **2013**, *110*, 085504.
16. Chen, L.; Feng, B. J.; Wu, K. H. Observation of a Possible Superconducting Gap in Silicene on Ag(111) Surface. *Appl. Phys. Lett.* **2013**, *102*, 081602.
17. Feng, B.; Li, H.; Liu, C. C.; Shao, T. N.; Cheng, P.; Yao, Y.; Meng, S.; Chen, L.; Wu, K. H. Observation of Dirac Cone Warping and Chirality Effects in Silicene. *ACS Nano* **2013**, *7* (10), 9049–9054.
18. Lin, C. L.; Arafune, R.; Kawahara, K.; Kanno, M.; Tsukahara, N.; Minamitani, E.; Kim, Y.; Kawai, M.; Takagi, N. Substrate-Induced Symmetry Breaking in Silicene. *Phys. Rev. Lett.* **2013**, *110*, 076801.
19. Fleurence, A.; Friedlein, R.; Ozaki, T.; Kawai, H.; Wang, Y.; Yamada-Takamura, Y. Experimental Evidence for Epitaxial Silicene on Diboride Thin Films. *Phys. Rev. Lett.* **2012**, *108*, 245501.
20. Friedlein, R.; Fleurence, A.; Sadowski, J. T.; Yamada-Takamura, Y. Tuning of Silicene-Substrate Interactions with Potassium Adsorption. *Appl. Phys. Lett.* **2013**, *102*, 221603.
21. Meng, L.; Wang, Y.; Zhang, L.; Du, S.; Wu, R.; Li, L.; Zhang, Y.; Li, G.; Zhou, H.; Hofer, W. A. H.; Gao, J. Buckled Silicene Formation on Ir(111). *Nano Lett.* **2013**, *13*, 685–690.
22. Chiappe, D.; Scalise, E.; Cinquanta, E.; Grazianetti, C.; van den Broek, B.; Fanciulli, M.; Houssa, M.; Molle, A. Two-Dimensional Si Nanosheets with Local Hexagonal Structure on a MoS_2 Surface. *Adv. Mater.* **2014**, *26*, 2096–2101.
23. Liu, Z. L.; Wang, M. X.; Liu, C.; Jia, J. F.; Vogt, P.; Quaresima, C.; Ottaviani, C.; Olivieri, B.; De Padova, P.; Le Lay, G. The Fate of the $(2\sqrt{3} \times 2\sqrt{3})R30°$ Silicene Phase on Ag(111). *APL Mater.* **2014**, *2*, 092513.
24. Prévot, G.; Bernard, R.; Cruguel, H.; Borensztein, Y. Monitoring Si Growth on Ag(111) with Scanning Tunneling Microscopy Reveals that Silicene Structure Involves Silver Atoms. *Appl. Phys. Lett.* **2014**, *105*, 213106.
25. Rahman, M. S.; Nakagawa, T.; Mizuno, S. Growth of Si on Ag(111) and Determination of Large Commensurate Unit Cell of High-Temperature Phase. *Jpn. J. Appl. Phys.* **2015**, *54*, 015502.
26. Tao, L.; Cinquanta, E.; Chiappe, D.; Grazianetti, C.; Fanciulli, M.; Dubey, M.; Molle, A.; Akinwande, D. Silicene Field-Effect Transistors Operating at Room Temperature. *Nat. Nanotechnol.* **2015**, *10*, 227–231.
27. Guo, Z. X.; Furuya, S.; Iwata, J. I.; Oshiyama, A. Absence and Presence of Dirac Electrons in Silicene on Substrates. *Phys. Rev. B: Condens. Matter Mater. Phys.* **2013**, *87*, 235435.
28. Jamgotchian, H.; Ealet, B.; Colignon, Y.; Maradj, H.; Hoarau, J.-Y.; Bibérian, J.-P.; Aufray, B. A Comprehensive Study of the $(2\sqrt{3} \times 2\sqrt{3})R30°$ Structure of Silicene on Ag(111). *arXiv: 1412.4902* **2015**; DOI: 10.1088/0953-8984/27/39/395002.

29. Qiu, J. L.; Fu, H. X.; Xu, Y.; Oreshkin, A. I.; Shao, T.; Li, H.; Meng, S.; Chen, L.; Wu, K. H. Ordered and Reversible Hydrogenation of Silicene. *Phys. Rev. Lett.* **2015**, *114*, 126101.

30. Osborn, T. H.; Farajian, A. A.; Pupysheva, O. V.; Aga, R. S.; Lew Yan Voon, L. C. *Ab Initio* Simulations of Silicene Hydrogenation. *Chem. Phys. Lett.* **2011**, *511*, 101–105.

31. Lew Yan Voon, L. C.; Sandberg, E.; Aga, R. S.; Farajian, A. A. Hydrogen Compounds of Group-IV Nanosheets. *Appl. Phys. Lett.* **2010**, *97*, 163114.

32. Houssa, M.; Scalise, E.; Sankaran, K.; Pourtois, G.; Afanas'ev, V. V.; Stesmans, A. Electronic Properties of Hydrogenated Silicene and Germanene. *Appl. Phys. Lett.* **2011**, *98*, 223107.

33. Zheng, F. B.; Zhang, C. W. The Electronic and Magnetic Properties of Functionalized Silicene: a First-Principles Study. *Nanoscale Res. Lett.* **2012**, *7*, 422.

34. Huang, B.; Deng, H. X.; Lee, H.; Yoon, M.; Sumpter, B. G.; Liu, F.; Smith, S. C.; Wei, S. H. Exceptional Optoelectronic Properties of Hydrogenated Bilayer Silicene. *Phys. Rev. X* **2014**, *4*, 021029.

35. Zhao, J.; Petek, H. Non-Nuclear Electron Transport Channels in Hollow Molecules. *Phys. Rev. B: Condens. Matter Mater. Phys.* **2014**, *90*, 075412.

36. Perdew, J. P.; Burke, K.; Ernzerhof, M. Generalized Gradient Approximation Made Simple. *Phys. Rev. Lett.* **1996**, *77*, 3865.

37. Kresse, G.; Furthmüller, J. Efficient Iterative Schemes for *Ab Initio* Total-Energy Calculations Using a Plane-Wave Basis Set. *Phys. Rev. B: Condens. Matter Mater. Phys.* **1996**, *54*, 11169.